

## COMPUTATIONAL FLUID DYNAMICS MODELLING OF CHEMISTRY REACTION SCHEMES IN A LAB-SCALE OXY-FUEL FURNACE

Audai Hussein AL-ABBAS<sup>a,b</sup>, Jamal NASER<sup>a\*</sup>, and Aaron BLICBLAU<sup>a</sup>

<sup>a</sup>Faculty of Engineering & Industrial Sciences, Swinburne University of Technology, Hawthorn 3122, AUSTRALIA

<sup>b</sup>Technical College of Al-Musaib, Commission of Technical Education, Babylon, IRAQ

\*Corresponding author, E-mail address: jnaser@swin.edu.au

### ABSTRACT

This paper presents a three-dimensional numerical investigation of pulverized dry lignite in a 100 kW oxy-fuel furnace. A computational fluid dynamics (CFD) code was used to model four different combustion scenarios. One air-fired combustion case and three oxy-fuel-fired cases, known as OF25 (25 vol. % O<sub>2</sub> concentration), OF27 (27 vol. % O<sub>2</sub> concentration), and OF29 (29 vol. % O<sub>2</sub> concentration), were modelled. User-defined functions (UDFs) for the multistep reaction schemes were written and incorporated to the CFD code. Under oxy-fuel combustion, the appropriate mathematical models were implemented to calculate the flame temperature distributions and species concentrations (O<sub>2</sub> and CO<sub>2</sub>). The multi-step chemical reaction schemes were used for the gas-phase and solid-phase coal particle reactions. In addition to the one-step (reference) reaction scheme, two-step and three-step reaction schemes were considered in this numerical study. Compared to the one-step and two-step reactions, the three-step reaction results showed a reasonably good agreement against the experiments for all combustion cases. This numerical investigation of the oxy-fuel combustion scenarios might probably provide significant information towards modelling of large-scale oxy-fuel-fired coal tangentially furnaces/boilers.

### NOMENCLATURE

$\rho$	density
$\Phi$	variables
$U$	velocity
$\Gamma$	diffusion coefficient
$S_{\Phi}$	source term

### Abbreviations

UDFs	user-defined functions
GHG	greenhouse gases
PC	pulverized coal
RFG	recycled flue gas
PDE	partial differential equation
DTRM	discrete transfer radiation method
WSGGM	weighted sum of gray gases model

### INTRODUCTION

Emissions from fossil fuel combustion, particularly coal-firing, have increased in recent years. The coal power plants have been considered the main source of energy in many countries due to the low-cost of coal (Achim et al., 2009; Dodds et al., 2011; Dodds and Naser, 2012). It is a cost effective source of energy among the other available

alternative sources. However, coal is a major contributor to the greenhouse gas (GHG) emissions and hence global climate change. Carbon dioxide (CO<sub>2</sub>) and nitric oxides (NO<sub>x</sub>) are the main GHGs from the coal fired power station. Research on coal combustion can play an important role for developing clean energy from coal (Ahmed et al., 2007; Ahmed and Naser, 2011; Hart and Naser, 2009).

Recently, several CO<sub>2</sub> capture techniques, such as pre-combustion capture, post-combustion capture, and oxy-fuel combustion, have been developed. The last CO<sub>2</sub> capture technique, which can be written as O<sub>2</sub>/CO<sub>2</sub>, has been widely considered the most appropriate option to reduce the harmful gases from pulverized coal (PC) power plants (Buhre et al., 2005; Kanniche et al., 2009; Wall et al., 2009). In oxy-fuel combustion the partial pressure of carbon dioxide in the flue gas is increased help to make its sequestration and compression processes easier and more economical. In this technique, a mixture of pure oxygen and recycled flue gas (RFG) is used instead of air in the combustion chamber (Kakaras et al., 2007). Either wet or dry RFG can be used. A higher concentration of CO<sub>2</sub> is then achieved in the flue gas. Under the O<sub>2</sub>/CO<sub>2</sub> combustion technique, flame temperature levels, species concentrations and radiation heat transfer may vary with respect to the air-fired case. These changes on the combustion characteristics are principally due to the higher volumetric heat capacity of CO<sub>2</sub> relative to that of N<sub>2</sub> in the air-fired case, radiative properties of gas mixture, and other gas properties such as kinetic viscosity, thermal diffusivity, and gas phase chemistry (Al-Abbas et al., 2011; Al-Abbas and Naser, 2012).

Before switching to an oxy-fuel combustion approach for a conventional large-scale boiler, lab-scale furnaces have to be initially examined under several oxy-fuel combustion conditions. This strategy of examination is strongly recommended to investigate the combustion characteristics and boiler performance under the challenging O<sub>2</sub>/CO<sub>2</sub> scenarios.

The CFD modelling studies can provide a wide range of information for the design of furnace and burner. And this can reduce the cost of time-consuming experimental investigations. The flame structure, gas temperatures distributions, chemical species concentrations, radiative heat transfer etc., can be numerically predicted under different combustion conditions (Al-Abbas and Naser, 2012).

Until now there has been very little research conducted on the dry lignite oxy-fuel combustion using multi-steps reaction schemes in detail for volatile and residual char combustion. In this paper, the gaseous and solid phase

chemistry mechanisms are presented. Multi-steps reaction schemes were carried out in four different combustion scenarios on a lab-scale 100 kW furnace. The AVL ire CFD (AVL (2011)) code was used to model the air-fired and three different oxy-fuel combustion scenarios (known as OF25, OF27, and OF29). The flame temperature distributions and species concentrations (O<sub>2</sub>, CO, and CO<sub>2</sub>) inside the furnace were presented and validated against the experimental data of Andersson (2007) for one-, two-, and three-step reactions. This investigation by the authors is followed up in their detailed study (Al-Abbas and Naser, (2012)).

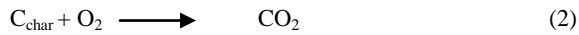
### MULTI-STEP REACTION SCHEMES

In this study, volatile, char, O<sub>2</sub>, N<sub>2</sub>, CO<sub>2</sub>, CO, H<sub>2</sub>, and H<sub>2</sub>O were considered and taken into account in three different chemical reaction schemes. In the previous numerical study of Al-Abbas et al. (2011), the one-step reaction results showed some discrepancies in terms of temperature distributions and species concentrations against the measured data. The authors concluded that the numerical results could be highly improved, particularly in the combustion zone if the intermediate species are considered and taken into account. This requires the usage of multi-step reactions in both the gas-phase and solid-phase combustions. The multi-step chemical reaction schemes can provide good information to clarify the connection of the order of reaction of char burnout and CO/CO<sub>2</sub> production rate with the temperature and oxygen partial pressure (Nikolopoulos et al. 2011; Hurt and Calo 2001). For the oxy-coal combustion, the following chemical equations of one-, two-, and three-step reaction schemes were considered:

For the homogenous phase, the chemical equation of devolatilized methane burned with oxygen can be given:



For the heterogeneous phase, the chemical equation of char burned with oxygen can be given as follows:



The heats of combustion of Eqs. (1) and (2), taken into account in the combustion model, were equal to -802310 kJ/kmol. and -393520 kJ/kmol., respectively.

The two-step reaction scheme provided improved information accounting for the carbon monoxide in the gaseous reaction and the char burn-out reaction, as shown in the following chemical equations:

For the homogenous phase, the chemical equations of devolatilized methane burned with oxygen can be expressed by the following reactions:



While the chemical equation for char burned with oxygen can be given as follows:



The reverse chemical reaction of Eq. (4) has an important effect on the concentration of CO and the level of flame

temperature inside the furnace. The heats of reaction of first and second equations in the two-step reaction scheme (homogenous phase) are 307880 kJ/kmol and -1110190 kJ/kmol, respectively.

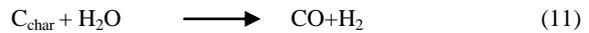
The three-step reaction scheme can predict well the intermediate species (CO and H<sub>2</sub>) and the main species (CO<sub>2</sub> and H<sub>2</sub>O). Thus, the devolatilized methane and residual char (C<sub>char</sub>) are presented in three-step chemical reaction in order to precisely elucidate the thermal dissociation mechanism of the main species, as shown in the following reactions.

For the homogenous phase, the chemical equations of devolatilized methane burned with oxygen can be expressed in the three chemical reactions:



The heats of reaction of first, second, and third chemical equations in this reaction scheme are 549710 kJ/kmol, -868360 kJ/kmol, and -483660 kJ/kmol, respectively.

For the heterogenous phase, the chemical equations of char burned with oxygen, carbon dioxide, and water vapour can be expressed as follows:



The heats of combustion of the above-mentioned species are taken into account and incorporated as a source term in the enthalpy equation for all combustion cases as separate subroutines.

### MODEL DESCRIPTION

A CFD code, AVL(2011)fire version 2008, was used in this numerical study to model four combustion cases in a 100 kW furnace. The volumetric flow rates of oxidizers in the burner were reduced for the OF25, OF27, and OF29 combustion cases by 17%, 23%, and 28%, respectively compared with that of the air-fired case. The schematic diagram of the furnace geometry is given in Figure 1. The UDFs were written and incorporated into the CFD code for devolatilization, char burnout, and heat transfer models. In addition, many sub-models are coupled through the source terms of the partial differential equation (PDE), and it can be given as follows:

$$\frac{\partial}{\partial t}(\rho\Phi) + \frac{\partial}{\partial x_i}(\rho U_i \Phi) = \frac{\partial}{\partial x_i} \left( \Gamma \frac{\partial \Phi}{\partial x_i} \right) + S_\Phi + S_{\rho\Phi} \quad (12)$$

For the turbulence model, the standard k- $\epsilon$  model has been used. The discrete transfer radiation method (DTRM) was implemented for the heat transfer model. While the weighted sum of gray gases model (WSGGM) was selected for the gas radiation calculation in this oxy-fuel combustion study. The combination between the velocity and pressure has been calculated by the SIMPLE algorithm. A grid-independent test was carried out, and it noted that the changes observed in numerical results were

very marginal, and therefore the 224,000 grid system was selected in this numerical simulation.

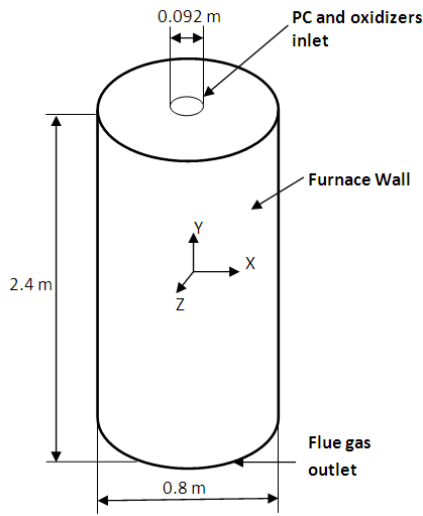


**Figure 1:** Schematic diagram of the furnace geometry.

## RESULTS

The flame temperature distributions at four different horizontal locations and along the upper half of the furnace axis for the air-fired (reference) and oxy-fuel (OF25) combustion cases are presented in Figure 2a. The length of the flame was higher for the air-fired case compared to the oxy-fuel (OF25) case. It can also be seen that the flame structure of the OF25 case showed some similarities, but is a bit shorter than the air-fired case. It is clearly evident at the horizontal location of the furnace at  $Y=40$  cm. For both combustion cases, the width of the flame at locations  $Y=65$ ,  $82$ , and  $98$  cm was approximately identical. Compared to the OF25 flame, the value of flame temperature of the reference combustion case was higher due to the recycled  $\text{CO}_2$  used in the oxy-fuel case that led to the absorption of heat from the flame. This is because of the higher specific heat capacity of  $\text{CO}_2$  with respect to that of  $\text{N}_2$ , as explained earlier.

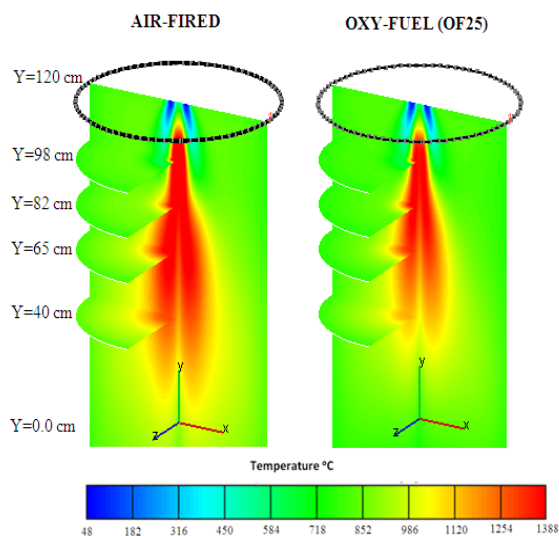


**Figure 2a:** Distributions of flame temperature ( $^{\circ}\text{C}$ ) for the air-fired and oxy-fuel-fired (OF25) cases at the upper half of the furnace.

In Figure 2b, the flame temperature ( $^{\circ}\text{C}$ ) distributions for oxy-fuel combustion cases (OF27 and OF29) are presented. The OF27 and OF29 flames are visibly shorter, and they are confined in the vicinity of the burner exit plane compared to that of the combustion cases in Figure 2a. Additionally, the flames of OF27 and OF29 are wider compared to the air-fired and OF25 cases, as evident at  $Y=82$  and  $98$  cm. Regarding the flame temperatures, it can be seen that the OF29 and OF27, in Figure 2b, have the higher temperature levels compared to that of air-fired and OF25 cases (Figure 2a). The structure of the OF25 flame is closer to that of the air-fired case. The RFG and  $\text{O}_2$  concentrations adopted in all oxy-fuel cases are the main reasons for these differences in the shapes and levels of flame temperatures.

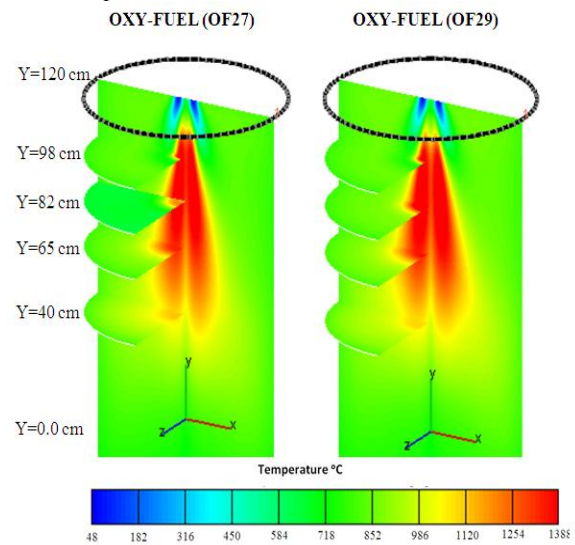
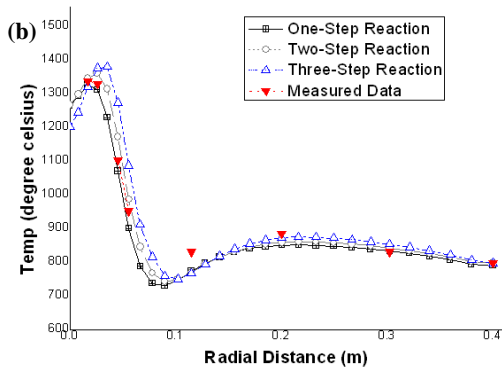
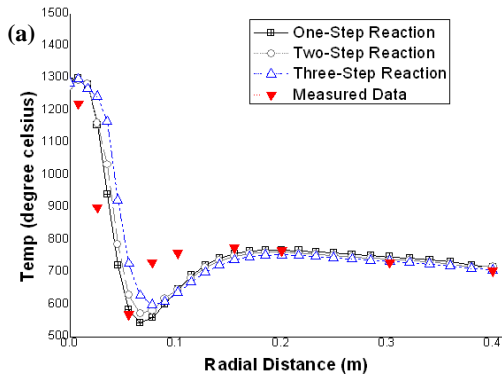
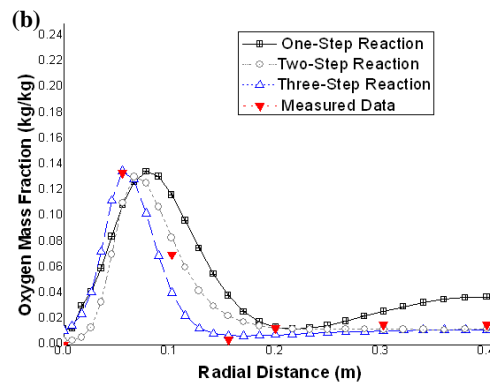
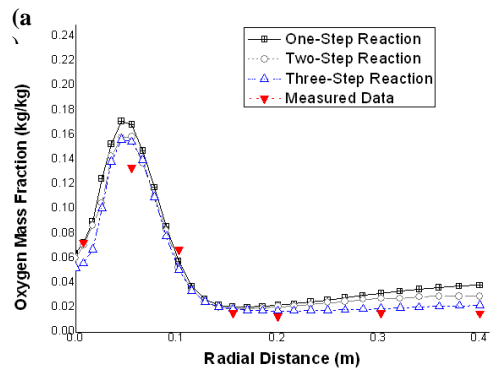


**Figure 2b:** Distributions of flame temperature ( $^{\circ}\text{C}$ ) for the oxy-fuel combustion (OF27 and OF29) cases at the upper half of the furnace.

Figures 3 a and b presents the comparison of the predicted temperature distributions ( $^{\circ}\text{C}$ ) with the measured data at  $Y=98$  cm by using one-, two-, and three-step chemical reaction schemes for the air-fired and oxy-fuel (OF29) combustion cases, respectively. In Figs. 3 a and b, the two- and three-step reaction schemes give better predictions of temperature profiles, especially in region close to the furnace wall in comparison to the results of the one-step reaction scheme. This can be explained by three main reasons. Firstly, in this region of the furnace, the predictions obtained with multiple reaction schemes also showed good comparisons of oxygen concentrations with the experiments as shown in Figures 4a and b. This improvement of  $\text{O}_2$  concentrations is highly affected on the combustion characteristics, and therefore led to improved flame temperature distributions. Secondly, in the near wall region, the swirl effect by the primary and secondary registers has less aerodynamic effect compared to the near-burner region. Thirdly, due to the formation of  $\text{CO}$  and  $\text{H}_2$  in the combustion zone obtained with the multi-step reaction schemes. Thus, the combustion heat is gradually released causing a drop in the highest flame temperature.



**Figures 3 a and b:** Temperature distribution ( $^{\circ}\text{C}$ ) profiles between the predicted results and measured data at  $Y=98$  cm from the middle point of the furnace in one-, two-, and three-step reaction schemes for the air-fired and OF29 combustion cases, respectively.



**Figures 4 a and b:** Oxygen mass fraction (kg/kg) profiles between the predicted results and measured data at  $Y=98$  cm from the middle point of the furnace in one-, two-, and

three-step reaction schemes for the air-fired and OF29 combustion cases, respectively.

Figure 5 presents the  $\text{CO}_2$  concentration for the air-fired and OF29 combustion cases in the upper quarter of the furnace (from 0.0 to 600 mm in the axial direction). In Figure 5, the results obtained from the three-step reaction scheme are used. The higher values of the carbon dioxide were 17% and 90% (kg/kg) for the air-fired and OF29 combustion cases, respectively. These numerical results were very consistent with the experimental results.

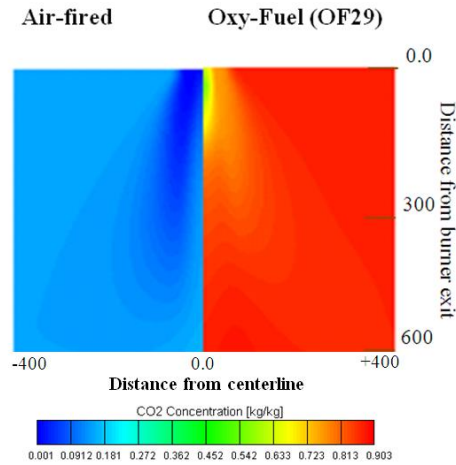
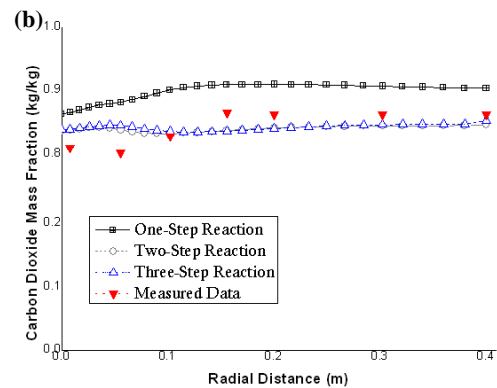
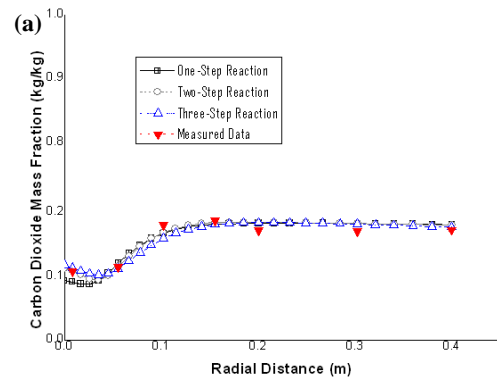


**Figure 5:** Distributions of  $\text{CO}_2$  concentrations for the air-fired (left-hand side) and OF29 (right-hand side) combustion cases from the burner exit plane (0.0 mm) to 600 mm in the axial direction of the furnace.



**Figures 6 a and b:** Comparisons of the  $\text{CO}_2$  mass fraction (kg/kg) profiles between the predicted results and measured data at  $Y= 82$  cm for the air-fired and oxy-fuel (OF29) cases in one-, two-, and three-step reaction schemes.

In Figures 6a and b, the validation of the predicted results with the experiments are presented in one-, two-, and three-step reaction schemes at Y=82 cm from the central furnace point. The results showed a good agreement with the measured data, particularly in two- and three-step reactions. The results of the one-step reaction were slightly over predicted, especially in the OF29. This could be due to increasing the O<sub>2</sub> concentration in the gas mixture.

## CONCLUSION

CFD was used to predict and analyze four different combustion scenarios (air-fired, OF25, OF27, and OF29), simulating the experiments on a 100 kW Chalmers' lab-scale furnace. The temperature distributions and species concentrations (O<sub>2</sub> and CO<sub>2</sub>) were presented at different locations in the furnace. The one-, two-, and three-step chemical reaction schemes were carried out on the gas-phase and solid-phase of the pulverized lignite particles. The predicted results showed good agreements with the measured data for all combustion cases, particularly with the three-step reaction scheme. This is because of the adoption of dissociation mechanisms of species in the multi-step reaction schemes. These numerical observations are significant and should be taken into account of calculations during modelling oxy-fuel large-scale coal combustion furnaces.

## REFERENCES

- ACHIM, D., NASER, J. MORSI, Y.S., PASCOE, S., (2009), "Numerical investigation of full scale coal combustion model of tangentially fired boiler with the effect of mill ducting", *Heat and Mass Transfer*, 1-13.
- AHMED, S., and NASER, J., (2011), "Numerical investigation to assess the possibility of utilizing a new type of mechanically thermally dewatered (MTE) coal in existing tangentially-fired furnaces", *Heat and Mass Transfer*, 47, 457-469.
- AHMED, S., HART, J., NIKOLOV, J., SOLNORDAL, C., YANG, W., NASER, J., (2007), "The effect of jet velocity ratio on aerodynamics of a rectangular slot-burner in the presence of cross-flow", *Experimental Thermal and Fluid Science*, 32, 362-374.
- AL-ABBAS, A.H., NASER, J., DODDS. D., (2011), "CFD modelling of air-fired and oxy-fuel combustion of lignite in a 100 kW furnace", *Fuel*, 90, 1778-1795.
- AL-ABBAS, A.H., and NASER, J., (2012), "Effect of Chemical Reaction Mechanisms and NO<sub>x</sub> Modeling on Air-Fired and Oxy-Fuel Combustion of Lignite in a 100-kW Furnace", *Energy & Fuels*, 26, 3329-3348.
- ANDERSSON, K., (2007), "Characterization of oxy-fuel flames - their composition, temperature and radiation", PhD Thesis, Chalmers University of Technology, Göteborg.
- AVL Fire CFD (2011) Solver v 8.5 manual, A-8020 Gras, Austria, www.avl.com, accessed 2011
- BUHRE, B.J.P., ELLIOTT, L.K., SHENG, C.D., GUPTA, R.P., and WALL, T.F., (2005), "Oxy-fuel combustion technology for coal-fired power generation", *Progress in Energy and Combustion Science*, 31, 283-307.
- DIEZ, L.I., CORTES, C., and PALLARES, J., (2008), "Numerical investigation of NO<sub>x</sub> emissions from a tangentially-fired utility boiler under conventional and overfire air operation", *Fuel*, 87, 1259-1269.
- DODDS, D., NASER, J., STAPLES, J. BLACK, C., MARSHALL, L., and NIGHTINGALE, V., (2011), "Experimental and numerical study of the pulverised-fuel distribution in the mill-duct system of the Loy Yang B lignite fuelled power station", *Powder Technology*, 207, 257-269.
- DODDS. D., NASER, J., (2012), "Numerical study of the erosion within the pulverised-fuel mill-duct system of the Loy Yang B lignite fuelled power station", *Powder Technology*, 217, 207-215.
- HART, J.T. NASER, J.A. WITT, P.J., (2009), "Aerodynamics of an isolated slot-burner from a tangentially-fired boiler", *Applied Mathematical Modelling*, 33, 3756-3767.
- HURT, R.H. and CALO, J.M., (2001), "Semi-global intrinsic kinetics for char combustion modelling", *Combustion and Flame*, 125, 1138-1149.
- KAKARAS, E., KOUMANAKOS, A., DOUKELIS, A., GIANNAKOPOULOS, D., VORRIAS, I., (2007), "Oxyfuel boiler design in a lignite-fired power plant", *Fuel*, 86, 2144-2150.
- KANNICHE, M., GROS-BONNIVARD, R., JAUD, P., VALLE-MARCOS, J. AMANN, C. BOUALLOU, (2009), "Pre-combustion, post-combustion and oxy-combustion in thermal power plant for CO<sub>2</sub> capture:", *Applied Thermal Engineering*, 30, 53-62.
- NIKOLOPOULOS, N., NIKOLOPOULOS, A., KARAMPINIS, E., GRAMMELIS, P. KAKARAS, E., (2011), "Numerical investigation of the oxy-fuel combustion in large scale boilers adopting the ECO-Scrub technology", *Fuel*, 90, 198-214.
- WALL, T., LIU, Y., SPERO, C., ELLIOTT, L., KHARE, S., RATHNAM, R. ZEENATHAL, F., MOGHTADERI, B. B. BUHRE, C. SHENG, R. GUPTA, T. YAMADA, K. MAKINO, J. YU, (2009), "An overview on oxyfuel coal combustion--State of the art research and technology development", *Chemical Engineering Research and Design*, 87, 1003-1016.